Frequency Domain Modeling of Non-laminated Cylindrical Magnetic Actuators

Lei Zhu, Carl R. Knospe, and Eric H. Maslen
Department of Mechanical and Aerospace Engineering
122 Engineers Way
University of Virginia
Charlottesville, VA 22903
lz5z@virginia.edu
crk4y@virginia.edu
ehm7s@virginia.edu

ABSTRACT

This paper presents an analytical approach to modeling the relationship between applied magnetomotive force and mechanical force produced for a non-laminated cylindrical magnetic actuator. The approach is based on dividing the actuator into elements according to the flux distribution inside the actuator, and finding the frequency-dependent reluctance of the flux paths of each element. An analytic model and its half order simplification are derived, both of which are explicitly dependent on actuator material and geometric properties. Performance predictions from both analytic models are compared with finite element analysis, demonstrating the accuracy of the models.

1. INTRODUCTION

Non-contact magnetic actuators can be of great benefit to many industrial applications. In many of these applications, the flotor (the levitated part) will not be composed of laminations, as this would be contradictory to the levitation's purpose (e.g., sheet metal conveyance). In others, cost or strength concerns preclude the use of laminations in either the flotor or the stator (the electromagnet). For example, thrust magnetic bearings in rotating machinery rarely have a laminated construction. Faraday's law dictates that eddy currents will appear in a non-laminated actuator whenever a changing current is applied. These eddy currents generate a magnetic field that opposes the change in field generated by the varying actuator coil current, causing a reduction in the electromagnetic force produced, and resulting a slower change in the force than that in the current. As a result, eddy currents have a fundamental impact on the dynamic stiffness and servo bandwidth that can be attained by a magnetic suspension system. An accurate analytic model of the eddy current effect would be highly beneficial during the design stage to determine the impact of actuator geometric and material properties on suspension performance. For example, such knowledge could clearly be used in design optimization.

Several studies have been done to develop analytic models for non-laminated magnetic actuators of different types. Zmood [1] used a one-dimensional eddy current formulation for laminated magnetic circuits described in [2] to model a non-laminated C type magnetic actuator having a large ratio of pole width to height. Zmood applied a one-term expansion of the formulation and derived a first order analytic model. Feeley [3] used a two-dimensional eddy current formulation for a long rectangular bar presented in [2] to model a non-laminated C type magnetic actuator with pole width and height of the same order of magnitude. After neglecting the summation term in the formulation, Feeley applied an *ad hoc* approximation that resulted in a half order analytic model. In both these papers, the authors assume as a matter of course that the profile of flux density in a cross section of the air gap is the same as that in the associated cross section of pole iron. This is a reasonable assumption for static analysis but not for harmonic because of eddy currents. Kucera and Ahrens [4] examined a non-laminated cylindrical magnetic actuator. They divided the actuator into elementary geometric forms, and used the solution of the Maxwell's equations for a semi-infinite plate in approximating the flux distribution in each part. From this, they developed a generalized form of the flux equation similar to the one-dimensional eddy current formulation in [2], combined the various part models, and derived an analytic model. Since it was assumed that the air gap flux density had a uniform distribution that was independent of the frequency of the harmonic field, this model does not allow changes

in the spatial variation with frequency. Furthermore, a parameter in this analytic model must be identified from experimental data, as it does not correspond to any geometric or material property of the actuator. Thus, this result is not well suited to actuator design optimization.

The non-laminated cylindrical magnetic actuator studied in this paper is composed of three parts, a stator, a flotor and a coil shown in Fig. 1. The actuator geometry is axisymmetric, as is the flux distribution inside the actuator. Fig. 2 displays the cross-section with all the dimensional notations. Throughout this paper, we will use a cylindrical coordinate system (*r, z,* φ).

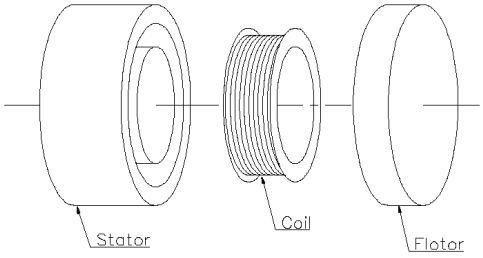

Fig. 1: Exploded View of the Cylindrical Magnetic Actuator

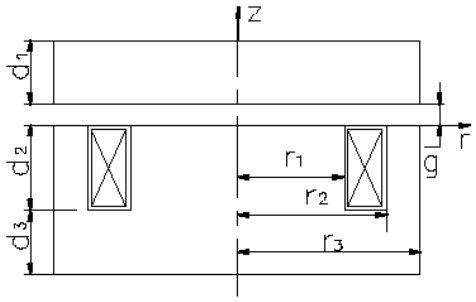

Fig. 2: The Cross Section of the Magnetic Actuator

The goal of this paper is to determine the transfer function from applied magnetomotive force to mechanical force produced for a non-laminated cylindrical magnetic actuator such as shown in Fig. 1. Hysteresis, saturation, leakage, and fringing flux are beyond the scope, and only linear and isotropic materials are considered. The transfer function desired will be derived based on an extension of the conventional magnetic circuit theory [5].

2. ELEMENT EFFECTIVE RELUCTANCES

2.1 Reluctance for a Solid Iron in a Harmonic Field

Magnetic circuit theory [5] has been used quite successfully in the preliminary design of many electromagnetic devices. In this approach, the reluctance of a magnetic circuit for a static magnetic field is defined by

$$R = \frac{F}{\phi} \tag{1}$$

where $F=NI$ is the magnetomotive force, N is the number of turns of the primary coil, I is the current magnitude, and ϕ is the flux in the circuit. This formulation may also be employed for a harmonic field in well-laminated iron. If the materials used are all linear, then the reluctance of a certain element in the circuit possessing a uniform cross-sectional area normal to the flux can be expressed as

$$R = \frac{l}{\mu_r \mu_0 A} \tag{2}$$

where l is the length of the element in the direction of the flux, μ_r is the relative permeability, μ_0 is the permeability of free space, and A is the cross sectional area.

As mentioned in Section 1, we wish to employ magnetic circuit theory to develop an analytic model for a non-laminated cylindrical magnetic actuator. However, Equation (2) is not applicable in this context, as it does not take into account eddy current effects. In this section, we employ an example to illustrate how the definition in (1) can be extended to non-laminated iron with a harmonic magnetic field, and introduce a new notion of effective permeability that may be used to calculate the effective reluctance of the iron.

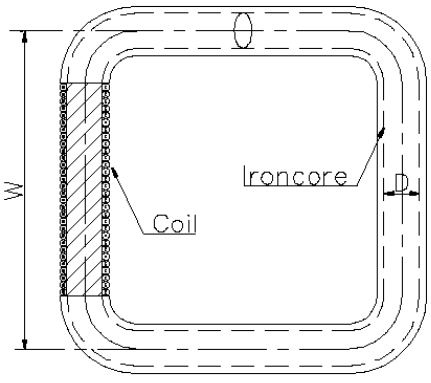

Fig. 3: The Solid Iron Core

Consider a solid iron core shown in Fig. 3 with a uniform circular cross section. A coil with N turns is evenly wound on the core. On the surface of the core, the field strength is $H_{sf}(s) = NI(s)/l$ with

$l = 4W$, and *I(s)* being the Laplace transform of the ac current *i(t)*. According to Lammeraner and Stafl [6], the flux density on each cross section is

$$B(s,r) = \mu_r \mu_0 H_{sf}(s) \frac{I_0(\alpha r)}{I_0(\alpha D/2)} \qquad (3)$$

$I_0(\cdot)$ is the zero order modified Bessel function of first kind;

$$\alpha = \sqrt{s\sigma\mu_r\mu_0} \qquad (4)$$

where σ is the electrical conductivity of the iron; and *s* is the complex frequency variable .

The flux in the iron core can be expressed as,

$$\phi(s) = \frac{NI(s)}{l} \int_0^{D/2} \mu_r \mu_0 \frac{I_0(\alpha r)}{I_0(\alpha D/2)} \cdot 2\pi r dr \qquad (5)$$

From (5), following the conventional definition in (1), we can define the reluctance of the iron core in a harmonic field to be

$$R_{eff}(s) = \frac{NI(s)}{\phi(s)} = \frac{l}{\int_0^{D/2} \mu_r \mu_0 \frac{I_0(\alpha r)}{I_0(\alpha D/2)} \cdot 2\pi r dr} \qquad (6)$$

This frequency-dependent reluctance R_{eff} is called the *effective reluctance* of the iron core.

Equation (3) shows that flux distribution inside the solid core is not uniform, and the spatial change of the distribution is due to the effect of eddy currents. Here, we reinterpret (3) as

$$B(s,r) = \mu_{eff}(s,r) H_{sf}(s) \qquad (7)$$

with $$\mu_{eff}(s,r) = \mu_r \mu_0 \frac{I_0(\alpha r)}{I_0(\alpha D/2)} \qquad (8)$$

Equation (7) interprets the spatial change of the flux distribution as being due to a spatial change of the material permeability. In this paper, the spatially changing permeability μ_{eff} is called the *effective permeability*. The definition of effective permeability in (8) is different from that provided elsewhere in the literature [5]. μ_{eff} can be used to calculated R_{eff} defined in (6). Since μ_{eff} is a spatial function, the effective reluctance of the core must be found by a limiting approach.

2.2 A Division of the Non-laminated Cylindrical Magnetic Actuator Geometry

As to motivate the approach taken, we will start our analysis by first considering some typical FEA results such as the one given in Fig. 4. These results show the following phenomena: (1) flux distributes mainly in a surface layer in the iron; the higher the frequency, the thinner this surface layer; (2) when flux leaves or enters the iron, there is a transition region near the surface where flux lines change direction; and (3) when the frequency is sufficiently high, the flux lines are either parallel to the *r* direction, or to the *z*-axis. This last phenomenon suggests that the actuator geometry can be divided into several elements, in each of which the flux distribution is only one-dimensional. Thus, modeling of an axisymmetric non-laminated magnetic actuator, which is normally considered as a two-dimensional problem, may be decomposed into several one-dimensional problems that are much easier to examine. That is, we may formulate the analysis problem like magnetic circuit theory [5]. Finally we draw the reader's attention to Fig. 5, which shows that the flux density in the air gap is not uniform at relatively low frequencies, and that its spatial variation changes with frequency and becomes quite significant at high frequency. For reasonable accuracy, it is necessary to consider this non-uniformity of air gap flux density in the modeling process

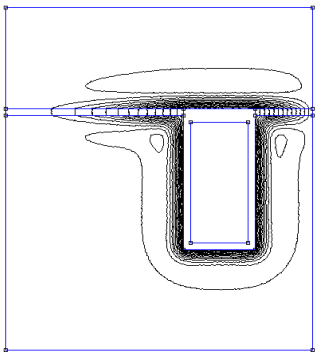

Fig. 4: The Harmonic Field at 50Hz

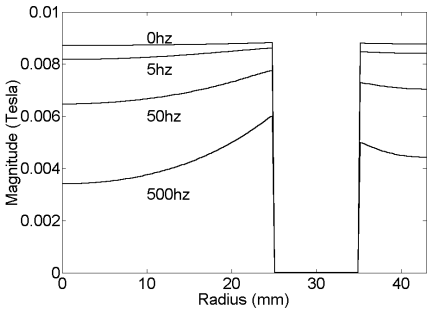

Fig. 5: The Magnitude of the Normal Flux Density in the Air Gap

Based on the directions of the flux lines and for the purpose of taking into account the non-uniformity of flux density in the air gap, the actuator geometry is divided into six elements as illustrated in Fig. 6. Given the simple flux distribution in each element, one can derive an effective permeability μ_{eff} from classic electromagnetic theory [7], and use it to calculate the effective reluctance for each element.

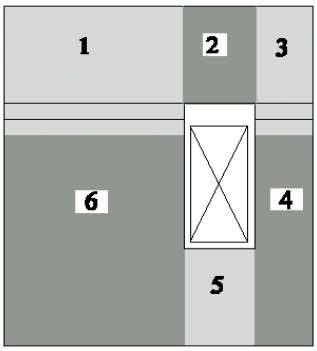

Fig. 6: The Division of the Geometry of the Magnetic Actuator

2.3 The Effective Reluctance of Each Element

For each element, we used a reluctance network model such as the one shown in Fig. 7 to find the effective reluctance. The effective reluctances for all the six elements are summarize in Table 1. Since they contain transcendental functions such as modified Bessel and hyperbolic tangential functions, which will not be suitable for design optimization or control purpose, simplification was carried out for each original effective reluctance. All the simplified reluctances are also given in Table 1.

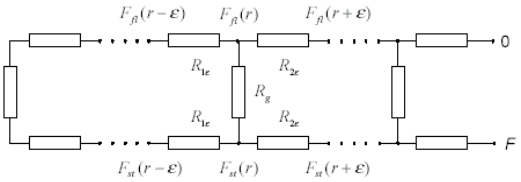

Fig. 7: The Reluctance Network Model for Element 1

3. ACTUATOR TRANSFER FUNCTION

The total effective reluctance of the actuator magnetic circuit may be calculated from the series interconnection of the elements as found in the previous section

$$R = \sum_{i=1}^{6} R_i \tag{9}$$

Hence, the transfer function from current to air gap flux is

$$\frac{\phi_g}{I_p} = \frac{N}{R} = \frac{N}{\sum_{i=1}^{6} R_i} \tag{10}$$

where N is the number of turns of the coil. Using Maxwell Stress Tensor [8], we found the transfer function from current to force:

$$\frac{F_p(s)}{I_p(s)} = \frac{\phi_b}{\mu_0}\left(\frac{1}{A_1}+\frac{1}{A_2}\right)\frac{N}{\sum_{i=1}^{6} R_i(s)} \tag{11}$$

I_p is the Laplace Transform of the perturbation current $i_p(t)$, and $\phi_b = NI_b \Big/ \sum_{i=1}^{6} R_i^0$ where I_b is the bias dc current, R_i^0 is the static value of R_i with $i = 1,2,\cdots,6$.

From the approximations chosen for the effective reluctances of the six elements summarized in Table 1, it is easy to see from the table that all the approximations are of the form

$$\widetilde{R}_i = R_i^0 + c_i\sqrt{s} \tag{12}$$

where $\widetilde{R}_i$ is the approximation of the effective reluctance R_i of element *i*; the coefficient of the half order term c_i is given in Table 1. Therefore, the total effective reluctance of the actuator R may be approximated as

$$\widetilde{R} = \sum_{i=1}^{6} \widetilde{R}_i = R^0 + c\cdot\sqrt{s} \tag{13}$$

where $\widetilde{R}$ is the approximation of the total effective reluctance R given in (9). Substitution of this approximation for the total effective reluctance into (10) and (11) yields a simplified model for the transfer functions of interest

$$\frac{\phi_g(s)}{I_p(s)} = \frac{N}{R^0 + c\cdot\sqrt{s}} \tag{14}$$

$$\frac{F_p(s)}{I_p(s)} = \frac{\phi_b}{\mu_0}\left(\frac{1}{A_1}+\frac{1}{A_2}\right)\frac{N}{R^0 + c\cdot\sqrt{s}} \tag{15}$$

The models of (92) and (93) are called fractional order systems [9].

Table 1: Effective Reluctances and Their Approximations

	Effective Reluctance $R_i(s)$	Approximation to Effective Reluctance $\widetilde{R}_i(s)$
1	$\frac{g\alpha_1 I_0(\alpha_1 r_1)}{2\pi\mu_0 r_1 I_1(\alpha_1 r_1)}$	$\frac{g}{\pi r_1^2 \mu_0} + \frac{1}{4\pi}\sqrt{\frac{\sigma}{\mu_r \mu_0}}\sqrt{s}$
2	$\frac{\ln(r_2/r_1)}{2\pi\mu_r\mu_0}\frac{\alpha}{\tanh(\alpha d_1)}$	$\frac{\ln(r_2/r_1)}{2\pi d_1\mu_r\mu_0} + \frac{\ln(r_2/r_1)}{2\pi}\sqrt{\frac{\sigma}{\mu_r\mu_0}}\sqrt{s}$
3	$\frac{g}{2\pi\mu_0 r_2}\cdot$ $\frac{\alpha_1[I_0(\alpha_1 r_2)K_1(\alpha_1 r_3)+K_0(\alpha_1 r_2)I_1(\alpha_1 r_3)]}{K_1(\alpha_1 r_2)I_1(\alpha_1 r_3)-I_1(\alpha_1 r_2)K_1(\alpha_1 r_3)}$	$\frac{g}{\pi\mu_0(r_3^2-r_2^2)} +$ $\frac{(2r_3^4\log\frac{r_3}{r_2}-\frac{3}{2}r_3^4+2r_2^2r_3^2-\frac{1}{2}r_2^4)}{2\pi(r_3^2-r_2^2)^2}\sqrt{\frac{\sigma}{\mu_r\mu_0}}\sqrt{s}$
4	$\frac{d_2}{2\pi\mu_r\mu_0 r_2}\cdot$ $\frac{\alpha[I_0(\alpha r_2)K_1(\alpha r_3)+K_0(\alpha r_2)I_1(\alpha r_3)]}{K_1(\alpha r_2)I_1(\alpha r_3)-I_1(\alpha r_2)K_1(\alpha r_3)}$	$\frac{d_2}{\pi\mu_r\mu_0(r_3^2-r_2^2)}+\frac{d_2}{2\pi r_2}\sqrt{\frac{\sigma}{\mu_r\mu_0}}\sqrt{s}$
5	$\frac{\ln(r_2/r_1)}{2\pi\mu_r\mu_0}\frac{\alpha}{\tanh(\alpha d_3)}$	$\frac{\ln(r_2/r_1)}{2\pi d_3\mu_r\mu_0}+\frac{\ln(r_2/r_1)}{2\pi}\sqrt{\frac{\sigma}{\mu_r\mu_0}}\sqrt{s}$
6	$\frac{d_2}{2\pi r_1\mu_r\mu_0}\frac{\alpha I_0(\alpha r_1)}{I_1(\alpha r_1)}$	$\frac{d_2}{\pi r_1^2\mu_r\mu_0}+\frac{d_2}{2\pi r_1}\sqrt{\frac{\sigma}{\mu_r\mu_0}}\sqrt{s}$

Equation (15) may be rewritten to show its dependence on electrical conductivity and relative permeability:

$$\frac{F_p(s)}{I_p(s)} = \frac{\beta_1}{(\beta_2\cdot\frac{1}{\mu_r}+\beta_3)\left((\beta_2\cdot\frac{1}{\mu_r}+\beta_3)+\sqrt{\frac{\sigma}{\mu_r}}\sqrt{s}\right)} \tag{16}$$

where coefficients $\beta_1, \beta_2,$ and β_3 are independent of σ and μ_r and are determined by actuator geometry only. The DC gain of (16) is $\beta_1\mu_r^2/(\beta_2+\beta_3\mu_r)^2$, the bandwidth is $\frac{\lambda(\beta_2+\beta_3\mu_r)^2}{\sigma\mu_r}$, and the gain-bandwidth is $\lambda\beta_1\frac{\mu_r}{\sigma}$, where $\lambda \equiv 2-\sqrt{3}$. Another recasting of (15) is

$$\frac{F_p(s)}{I_p(s)} = \frac{\beta_4}{(\beta_5+\beta_6 g)[(\beta_5+\beta_6 g)+\sqrt{s}]} \tag{17}$$

where coefficients $\beta_4, \beta_5,$ and β_6 are independent of the air gap length g. The DC gain of (17) is

$\beta_4/(\beta_5+\beta_6 g)^2$, the bandwidth is $\lambda\cdot(\beta_5+\beta_6 g)^2$, and the gain-bandwidth is $\lambda\beta_4$. As this discussion indicates, the bandwidth of an actuator increases with relative permeability at a rate that is no greater than linear while it increases in a quadratic fashion with respect to air gap. However, actuator gain-bandwidth is independent of air gap length.

4. COMPARISON WITH FEA

In this section, we compare the frequency responses of the complete analytic model (11) and the simplified analytic model (15) to that generated by finite element analysis for an actuator whose parameters are given below.

Table 2: Actuator Parameters

Parameters	Value
μ_r	1000
σ	2×10^6 Siemens/m
r_1	25mm
r_2	35mm
r_3	43mm
d_1	15mm
d_2	20mm
d_3	15mm
N	738
g	40mil

Fig. 8 demonstrates that the frequency responses of the two analytic models are very close to that of FEA

5. CONCLUSION

In this paper, an analytic model for a non-laminated cylindrical magnetic actuator including eddy current effects was developed. Due to the complexity of this complete analytic model, a simplified model was given. Both the complete and the simplified models are explicitly dependent on the actuator material and geometric properties. Thus, the influence of each of the actuator properties on its performance can be easily calculated. Comparison of the frequency responses of the two analytic models to that resulting from FEA demonstrates good accuracy. The analytical modeling approach employed in this paper is not limited to cylindrical actuators, and can be applied to non-laminated magnetic actuators of other geometries, such as C and E types.

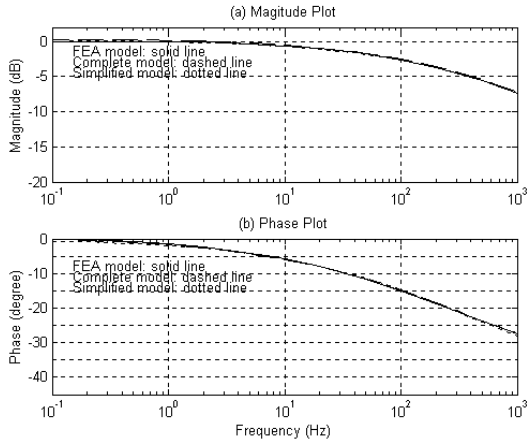

Fig. 8: A Model Comparison

Acknowledge

The author thanks National Science Foundation for support of this research, which was funded under Grant DMII-9988877.

References

[1] R. B. Zmood, D. K. Anand, and J. A. Kirk, "The influence of eddy currents on magnetic actuator performance." *Proc. IEEE* vol. 75, No.2, pp.259-260. Feb. 1987.

[2] R. L. Stoll, *The Analysis of Eddy Currents.* London: Oxford University Press, 1974

[3] J.J Feeley, " A simple dynamic model for eddy currents in a magnetic actuators." *IEEE Trans. Magnetics,* vol. 32, No.2, pp.453-458, Mar. 1996

[4] L. Kucera and M. Ahrens, "A Model for Axial Magnetic Bearings Including Eddy Currents", Proceedings of the Third International Symposium on Magnetic Suspension Technology, Tallahassee, Dec., 1995.

[5] M. A. Plonus, *Applied Electromagnetics*, McGraw-Hill, 1978

[6] J. Lammeraner and M. Stafl, *Eddy Currents*, Iliffe Books Ltd., 1966

[7] J. D. Jackson, *Classical Electrodynamics*, New York: Willey, Third Edition, 1999

[8] D. J. Griffiths. *Introduction to Electrodynamics.* New Jersey: Prentice-Hall, 1989.

[9] I. Podlubny, *Fractional Differential Equations.* San Diego: Academic Press, 1999